Calhoun
Institutional Archive of the Naval Postgraduate School

Calhoun: The NPS Institutional Archive

DSpace Repository

Faculty and Researchers | Faculty and Researchers' Publications

1997

Theory of high-gain free-electron lasers

Colson, W.B.

Nuclear Instruments and Methods in Physics Research A, Volume 393, (1997), pp. 82-85
http://hdl.handle.net/10945/44056

This publication is a work of the U.S. Government as defined in Title 17, United States Code, Section 101. Copyright protection is not available for this work in the United States.

Downloaded from NPS Archive: Calhoun

http://www.nps.edu/library

Calhoun is the Naval Postgraduate School's public access digital repository for research materials and institutional publications created by the NPS community. Calhoun is named for Professor of Mathematics Guy K. Calhoun, NPS's first appointed -- and published -- scholarly author.

Dudley Knox Library / Naval Postgraduate School
411 Dyer Road / 1 University Circle
Monterey, California USA 93943

Nuclear Instruments and Methods in Physics Research A 393 (1997) 82–85

NUCLEAR INSTRUMENTS & METHODS IN PHYSICS RESEARCH Section A

Theory of high-gain free-electron lasers

W.B. Colson

Physics Department, Naval Postgraduate School, Monterey, CA 93943, USA

Abstract

A powerful, coherent X-ray source may require a high-gain free-electron laser that makes use of self-amplified spontaneous emission. High gain can be achieved by using a combination of high peak current and a long undulator. The theoretical description of the high-gain FEL starts from the Lorentz–Maxwell equations solved self-consistently.

PACS: 41.60.C
Keywords: Free electron laser; X-rays

1. Introduction

Short-wavelength free-electron lasers (FELs) generating 1 Å X-rays appear feasible [1,2]. Since there are no X-ray mirrors, high gain is proposed as an attractive mechanism for generating coherent, powerful optical pulses. Some FEL designs make use of high harmonic numbers [3], but at the fundamental wavelength a large electron beam energy, like 5 GeV, is needed to reach the X-ray wavelengths. Because the large beam energy reduces coupling, achieving high gain requires a high-quality electron pulse of high peak current, like 5 kA, that is injected into a long undulator of around 50 m length.

About a decade ago, LLNL carried out a series of experiments with microwave and infrared FELs, ELF and PALADIN [4,5]. Both experiments operated well into the high-gain regime, but PALADIN's growth rate was dominated by poor beam quality. Even though these FELs produced much longer wavelengths, they are quite similar to the new X-ray FELs when described by dimensionless parameters.

The foundation of FEL theory calculates the microscopic electron evolution in the combined undulator and optical electric and magnetic fields. The relativistic Lorentz force and optical wave equations result in the electron pendulum [6] and slowly-varying wave [7] equations.

$$\mathring{\zeta} = \mathring{v} = |a|\cos(\zeta + \phi), \quad \mathring{a} = -j\langle e^{-i\zeta}\rangle, \tag{1}$$

where the dimensionless time is $\tau = 0 \to 1$ along the undulator, the dimensionless optical field is $a = |a|e^{i\phi}$, the electron phase ζ measures bunching on the optical wavelength scale, and the electron phase velocity is $v = \mathring{\zeta}$. Maxwell's wave equation, with a slowly varying amplitude and phase, defines the dimensionless current j, and $\langle \cdots \rangle$ is an average over sampled electrons in the beam. Each electron in the beam is identified by its initial conditions ζ_0 and v_0. The coupled pendulum and wave equations are valid for low gain $j \lesssim \pi$, high gain $j \gg \pi$, weak fields $|a| \lesssim \pi$, and strong fields $|a| \gg \pi$. Approximate values of the dimensionless current for real experiments are $j_{ELF} \approx 5000$ [4], $j_{PALADIN} \approx 2000$ [5], $j_{SLAC} \approx 5000$ [1], and $j_{DESY} \approx 10^4$ [2].

2. High-gain features

The fundamental properties of the high-gain FEL are determined by growth in weak optical fields [8–11]. Evolution in weak fields is characterized by small changes in the electron phase, $\Delta\zeta \ll \pi$. To zeroth order in the optical field strength $|a|$, the electron phase evolves as $\zeta(\tau) = \zeta_0 + v_0\tau$. Assume that all electrons in a monoenergetic beam start at resonance $v_0 = 0$, and that ζ_0 is distributed randomly such that $\langle e^{-i\zeta_0}\rangle \approx 0$. When expanded in weak optical fields, the coupled pendulum and wave equations reduce to $\mathring{\mathring{a}}(\tau) = ija(\tau)/2$. For small times $\tau \ll 1$, the optical field evolves slowly as $a(\tau) = a_0(1 + ij\tau^3/12 + \cdots)$. During the characteristic e-folding time, $\tau_j \approx 2/(\sqrt{3}(j/2)^{1/3}) \approx 0.1$, the electrons first become bunched with only small changes in the optical phase, then the field amplitude and the FEL gain $G(\tau) = |a(\tau)|^2/a_0^2 - 1$ grow exponentially, while the

0168-9002/97/$17.00 Copyright © 1997 Elsevier Science B.V. All rights reserved
PII S0168-9002(97)00432-4

optical phase $\phi(\tau)$ grows linearly in time:

$$G(\tau) \approx \exp[(j/2)^{1/3}\sqrt{3}\tau]/9, \qquad \phi(\tau) \approx (j/2)^{1/3}\tau/2, \qquad (2)$$

where the gain spectrum bandwidth is $\Delta\nu_0 \approx 2j^{1/3} \approx 10\pi$. The high-gain FEL interaction is collective, even without Coulomb forces, because all electrons communicate through the rapidly evolving optical field. The significant growth in the optical phase $\phi(\tau)$ is a crucial feature of the high-gain regime.

Fig. 1 shows the result of a simulation using Eq. (1) with current $j = 4000$, and initial field $a_0 = 0.01$. The electrons were initially spread uniformly in phase ζ_0 with a small Gaussian spread in initial phase velocities ν_0 of width $\sigma_G = 1$ about resonance. The gain $G(\tau)$ and phase evolution $\phi(\tau)$ along the undulator length $\tau = 0 \rightarrow 1$ are shown on the right, and agree with Eq. (2). Following the brief bunching time, $\tau_j \approx 0.1$, the figure shows the exponential gain $G(\tau) \approx e^{2\sqrt{2}\tau}/9$ and the linear growth in the optical phase $\phi(\tau) \approx 2\pi\tau$.

For an X-ray FEL, the initial field a_0 grows from shot noise [12–15]. With the short X-ray wavelength, there are only about 10^4 electrons within each section of the electron beam one wavelength of light long. One wavelength of light slips over the slower moving electrons as the electrons pass through each period of the undulator. During the e-folding time τ_j in an N period undulator, $N\tau_j \approx 10^2$ periods of information are exchanged between the optical field and $n_j \approx 10^6$ electrons in the beam. The shot noise contribution from these electrons results from their random initial phases ζ_0, and $|\tilde{a}(0)| \propto j\langle\cos\zeta_0\rangle \approx j/\sqrt{n_j}$. In simulations, it is not desirable to follow all the electrons in the beam and only a few hundred to a thousand are sampled. In order to simulate shot noise, the sampled electrons are spread uniformly in phase ζ_0 with a small additional random phase $\delta\zeta \ll \pi$ distributed as a Gaussian.

3. Beam quality degradation

The spread in the initial electron phase velocities ν_0 is determined by the initial energy and angular spreads in the beam. If the resulting spread in ν_0 is larger than $\sigma_j \approx j^{1/3} \approx 5\pi$, the exponential growth rate in weak optical fields can be degraded. Expanding Eq. (1) in weak fields again, but retaining a general electron distribution function $f(\nu)$ about ν_0, results in the FEL integral equation [16]

$$\tilde{a}(\tau) = \frac{ij}{2}\int_0^\tau d\tau'\,\tau' F(\tau') e^{-i\nu_0\tau'}\, a(\tau - \tau'), \qquad (3)$$

where $F(\tau') = \int d\nu f(\nu) e^{-i\nu\tau'}$ is the "characteristic function" of $f(\nu)$. A Gaussian distribution in $f(\nu)$ with standard deviation σ_G gives $F_G(\tau) = e^{-\sigma_G^2\tau^2/2}$, while an exponential distribution, characteristic of an angular spread in the electron beam, gives $F_\theta(\tau) = 1/(1 - i\sigma_\theta\tau)$. A symmetric $f(\nu)$ gives a real $F(\tau)$, while an asymmetric $f(\nu)$ gives a complex $F(\tau)$. For any spread, the amplitude of $F(\tau)$ decays in a characteristic time $\tau_\sigma \approx 1/\sigma$ in the integrand of Eq. (3) and degrades the growth rate of $a(\tau)$. The phase of $F(\tau)$ beats against $e^{-i\nu_0\tau}$ in the integrand of Eq. (3), and alters the resonance condition. The significance of the decay depends on its comparison to the characteristic growth time τ_j and the detailed shape of the distribution $f(\nu)$.

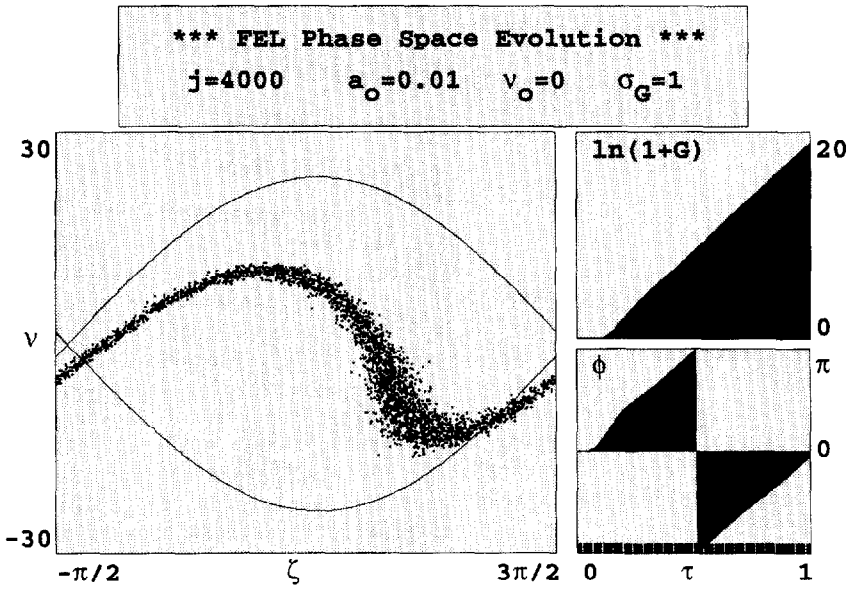

Fig. 1. Electron phase space, optical gain and phase evolution for high current.

For ELF, $\tau_j \approx \tau_\sigma \approx 0.1$ so that the experiment was affected by beam quality but still successful. For PALADIN, $\tau_\sigma \approx 0.03 < \tau_j \approx 0.1$ so that beam quality dominated the interaction causing a significantly reduced exponential growth rate. The proposed X-ray experiments anticipate comparable values for τ_j and τ_σ, like ELF. Whenever $\tau_j \lesssim \tau_\sigma \ll 1$, the FEL interaction is strongly dependent on the shape of the electron beam distribution $f(v)$. Experimenters work hard to improve beam quality, but often have little control over the shape of the resulting distribution function $f(v)$. Therefore, performance of the high-gain X-ray FELs proposed may be strongly dependent on conditions that are not controlled.

4. Strong field saturation

When the optical field becomes strong enough to cause the electron phase to evolve by as much as $\Delta\zeta \approx \pi$, the FEL interaction begins to saturate. The bunched electrons move from a phase where they amplify the optical field, to a phase where they can absorb energy back from the optical beam. Using the exponential form for the field (2) in the pendulum equation (1), the saturation field strength is found to be $a_s \approx 2(j/2)^{2/3}$ [17]. The FEL efficiency $\eta \approx (j/2)^{1/3}/2\pi N$ is the fraction of power extracted from the electron beam in a single pass. For ELF, $j \approx 5000$ and $N = 30$, so that $a_s \approx 120\pi$ and $\eta \approx 7\%$, as observed [4]. For SLAC, $j \approx 5000$ and $N = 1200$, so that $a_s \approx 200\pi$ and $\eta \approx 0.2\%$. Both ELF and the proposed SLAC X-ray FELs yield powerful GW pulses because of their powerful electron pulses.

After saturation, the trapped electron bunch continues to execute synchrotron oscillations at the synchrotron frequency $\nu_S = |a|^{1/2}$. In a longer undulator with many synchrotron oscillations, side bands may appear in the optical spectrum at $\pm \nu_S$ around the carrier wave. The proposed high-gain X-ray FELs are not long enough to observe the trapped-particle instability [17].

5. Optical guiding

In a 60 m long undulator, diffraction can cause the optical wave front to expand away from the small electron beam and diminish the interaction. Fortunately, the process of optical guiding focuses the wave front back into the electron beam with a mechanism comparable to fiber optics [18–21]. A theoretical analysis requires an extension of Eq. (1) to include diffraction of the complex optical field wave front in x and y [16]. The generalized wave equation is

$$\left[-\frac{i}{4}\nabla^2 + \frac{\partial}{\partial\tau}\right] a(x, y, \tau) = -\langle j e^{-i\zeta}\rangle_{(x,y,\tau)}, \tag{4}$$

where $\nabla_\perp^2 = \partial_x^2 + \partial_y^2$ describes the diffraction. In the absence of a driving current j, the optical phase of a freely diffracting wave front evolves as $\phi(\tau) = -\tau/z_0$ where z_0 is the dimensionless Rayleigh length. In the absence of diffraction, Eq. (2) shows that the optical phase evolves as $\phi(\tau) = (j/2)^{1/3}\tau/2$. The electron beam located in the middle of the diffracting optical wave front drives the optical phase opposite to that of natural diffraction and therefore acts to focus the light back into the beam area. The net result is similar to the effect of a glass fiber using a step or graded change in the index of refraction to focus the optical wave front. Optical guiding occurs in both strong and weak optical fields, and provides a dramatic effect crucial to extending the FEL interaction over long undulators.

The electron beam experiences betatron oscillations as it is focused back toward the center of the undulator axis by the higher magnetic fields off axis [17]. For the early ELF experiments, the number of betatron oscillations along the undulator length was large $n_\beta \approx NK/\gamma \approx 8$, while for the proposed X-ray FELs, the number of betatron oscillations is small $n_\beta \approx NK/\gamma \approx 0.2$, and negligible.

6. Optical coherence

Exploring the properties of optical coherence requires that Eq. (1) be extended in the longitudinal z direction instead of the transverse x, y directions, as in the last section. The optical field envelope now has a continuum of values along z, $a \to a_z$. The light, travelling at speed c, slips over the slower moving electrons, traveling at speed $c\beta_z$. In the slippage process, one wavelength of light passes over an electron as the electron passes through one period of the undulator. At a time τ, it is the electrons at site $z - \tau$ that interact with the optical field at site z. The generalized equations (1) are then [16]

$$\mathring{\zeta}_{z-\tau} = |a_z| \cos(\zeta_{z-\tau} + \phi_z),$$

$$\mathring{a}_z = -j_{z-\tau}\langle \exp(-i\zeta_{z-\tau})\rangle_{z-\tau}. \tag{5}$$

As an electron passes through each undulator period there are $w_e \approx 2\alpha K^2 \approx 0.1$ photons spontaneously emitted over a broad bandwidth, where $\alpha = \frac{1}{137}$ is the fine structure constant, and $K = e\bar{B}\lambda_0/2\pi mc^2 \approx 2$ is the undulator parameter. After the characteristic e-folding time $\tau_j \approx 0.1$, there are typically $N\tau_j w_e \approx 10$ photons emitted by each electron into a narrower bandwidth of fractional width $1/N\tau_j \approx 1\%$. In subsequent e-foldings, mode competition continues to narrow the spectrum around the fastest growing modes near resonance. The peak in the gain spectrum may be just above resonance because of the finiteness of the large j and electron beam quality [16]. During the slippage process, the electrons respond to the optical field in one part of the wave envelope and then drift back to drive another part. In this way, optical

phase information is exchanged along the wave envelope and long-range coherence develops. The spectral full-width at half-maximum is given by $\Delta\nu \approx \pi j^{1/6}\tau^{-1/2}$, and narrows as $\Delta\nu \propto \tau^{-1/2}$ along the undulator. The final spectral width is given by $\Delta\nu \approx \pi j^{1/6} \approx 4\pi$ for the X-ray experiments. This width is about the same as the spontaneous emission spectrum since $\Delta\lambda/\lambda \approx \Delta\nu/2\pi N \approx 0.2\%$. The advantage of the X-ray FEL is not that it has an exceptionally narrow spectrum, but that it has higher brightness, the optical power in the spectrum bandwidth [15,22].

7. Harmonics

When the undulator parameter is large enough, $K \gtrsim 1$, the electron motion in the linearly polarized undulator contains a fast z component, $k\Delta z \approx -\xi \sin(2k_0 z)$ where $\xi = K^2/2(1+K^2)$. The result of the fast longitudinal z motion is spontaneous emission and gain in odd higher-frequency harmonics $h = 1, 3, 5, \ldots$ An analysis of the FEL dynamics in harmonics shows that the form of Eq. (1) remains the same with a new dimensionless current density $j \rightarrow j_h$ [23],

$$j_h = jh[J_{(h+1)/2}(h\xi) + J_{(h-1)/2}(h\xi)]^2.$$

For the third harmonic $h = 3$, at one-third the fundamental wavelength, $j_{h=3} \approx 0.3j$ when $K \approx 1$, and $j_{h=3} \approx 0.8j$ when $K \approx 2$. The new values show substantial coupling and exponential growth when K is larger than unity. This is not hard to obtain and may be used in the SLAC experiment to reach the third harmonic and possibly shorter wavelengths. The difficulty in working at higher harmonics is increased sensitivity to the electron-beam quality. Bunching in the shorter wavelengths requires a smaller random component in the beam distribution. The third harmonic requires one-third the beam distribution width for the same performance as in the fundamental.

Acknowledgements

The authors are grateful for the support by the Naval Postgraduate School, and the Navy's Directed Energy Office.

References

[1] R. Tatchyn et al., Nucl. Instr. and Meth. A 375 (1996) 275.
[2] W. Brefeld et al., Nucl. Instr. and Meth. A 375 (1996) 295.
[3] X.J. Wang et al., Nucl. Instr. and Meth. A 375 (1996) 82.
[4] T. Orzechowski et al., Nucl. Instr. and Meth. A 250 (1986) 144.
[5] T. Orzechowski et al., Phys. Rev. Lett. 57 (1986) 2172.
[6] W.B. Colson, Phys. Lett. A 64 (1977) 190.
[7] W.B. Colson, S.K. Ride, Phys. Lett. A 76 (1980) 379.
[8] R. Bonifacio et al., Opt. Commun. 50 (1984) 373.
[9] W.B. Colson et al., Phys. Rev. A 34 (1986) 4837.
[10] R. Bonifacio et al., Phys. Rev. Lett. 73 (1994) 70.
[11] K.J. Kim, S.J. Hahn, Nucl. Instr. and Meth. A 358 (1995) 93.
[12] K.J. Kim, Nucl. Instr. and Meth. A 250 (1986) 396.
[13] K.J. Kim, Yu, Nucl. Instr. and Meth. A 250 (1986) 484.
[14] K. Krinsky, Yu, Phys. Rev. A 35 (1987) 3406.
[15] P. Pierini, W. Fawley, Nucl. Instr. and Meth. A 375 (1996) 332.
[16] W.B. Colson et al., Nucl. Instr. and Meth. A 259 (1987) 198; Nucl. Instr. and Meth. A 272 (1988) 386.
[17] W.B. Colson, Classical free electron laser theory, in: W.B. Colson, C. Pellegrini, A. Renieri (Eds.), Free Electron Laser Handbook ch. 5, North-Holland Physics, Elsevier, Netherlands, 1990, p. 115.
[18] D. Prosnitz, A. Szoke, G. Neil, Phys. Rev. A 24 (1981) 1436.
[19] C.M. Tang, P. Sprangle, Phys. Quantum Electron. 9 (1982) 627.
[20] G.T. Moore, Opt. Commun. 52 (1984) 45.
[21] T. Scharlemann, A. Sessler, J. Wurtele, Phys. Rev. 54 (1985) 1925.
[22] R. Bonifacio et al., Nucl. Instr. and Meth. A 341 (1994) 181.
[23] W.B. Colson, IEEE J. Quantum Electron. QE-17 (1981) 1417.